

Article

Pr@C₈₂ Metallofullerene: Calculated Isomeric Populations

Zdeněk Slanina^{1,2,*}, Filip Uhlík³, Takeshi Akasaka², Xing Lu² and Ludwik Adamowicz¹¹ Department of Chemistry and Biochemistry, University of Arizona, Tucson, AZ 85721-0041, USA² State Key Laboratory of Materials Processing and Die & Mould Technology, School of Material Science and Engineering, Huazhong University of Science and Technology, Wuhan 430074, China; lux@hust.edu.cn (X.L.)³ Department of Physical and Macromolecular Chemistry, Faculty of Science, Charles University in Prague, Albertov 6, 128 43 Praha, Czech Republic

* Correspondence: zdeneks@email.arizona.edu

Abstract: Relative equilibrium populations of the five lowest-energy isolated-pentagon-rule (IPR) isomeric structures of Pr@C₈₂ under high-temperature fullerene synthesis conditions were calculated with the Gibbs energy terms based on molecular characteristics derived using density functional theory (DFT) treatments (B3LYP/6-31+G*~SDD energetics and B3LYP/6-31G*~SDD entropy). Two leading isomers were identified, major Pr@C_{2v};9-C₈₂ and minor Pr@C_s;6-C₈₂. The calculated isomeric relative equilibrium populations agreed with observations.

Keywords: metallofullerenes; evaluations of isomeric populations; theory–experiment comparisons; quantum-chemical calculations

1. Introduction

Endohedral metallofullerenes have been pursued as not only targets of fundamental research but also promising species for nanoelectronics, as well as for energy conversions, superconductive properties, and applications in medicine. Such studies have also dealt with praseodymium-encapsulating metallofullerenes, in particular with Pr@C₈₂ [1–8] (a field-effect transistor was also fabricated [7] with one of its isomers). Actually, just two Pr@C₈₂ isomers (Figure 1) have been observed [3–6], namely the major species with the carbon cage obeying the isolated pentagon rule (IPR), conventionally labeled Pr@C_{2v};9-C₈₂, and the minor isomer Pr@C_s;6-C₈₂ (or Pr@C_s(c);6-C₈₂). Presently, there are two labeling or coding systems [9] for the IPR C₈₂ cages considered in this research. The older system works only with the symmetries of the cages (namely, the highest topological symmetries, regardless of possible symmetry reductions): C_{3v}(a), C_{3v}(b), C_{2v}, C₂(a), C₂(b), C₂(c), C_s(a), C_s(b), and C_s(c). The second labeling system employs serial numbers from the enumeration spiral algorithm [10]; these symbols are: C_{3v}(a);7, C_{3v}(b);8, C_{2v};9, C₂(a);3, C₂(b);1, C₂(c);5, C_s(a);2, C_s(b);4, and C_s(c);6. Numerous metals can be encapsulated in C₈₂ cages, frequently producing at least two isomers [4–6,9,11–16]. In the present report, the isomeric relative equilibrium populations (or the relative concentrations) were evaluated for the isomeric system of the five lowest-potential-energy Pr@C₈₂ IPR species, as such stability information is needed for the interpretation of some observations.

The relative stabilities of isomeric nanocarbons are mostly evaluated by simply using potential-energy terms. Nevertheless, several examples have been reported [17–26] showing that the Gibbs energy should be applied instead, as its entropy component becomes increasingly important at elevated temperatures. Consequently, an isomer that is not the lowest on the potential-energy scale can still exhibit the highest populations at the high temperatures needed for nanocarbon syntheses. Moreover, other higher-energy structures can in some cases exhibit relative stability interchanges with increasing temperature. Clearly enough, it is not possible to predict such relative stability interchanges simply from the potential-energy terms alone. Hence, computations were performed in this report for the



Citation: Slanina, Z.; Uhlík, F.; Akasaka, T.; Lu, X.; Adamowicz, L. Pr@C₈₂ Metallofullerene: Calculated Isomeric Populations. *Inorganics* **2023**, *11*, 313. <https://doi.org/10.3390/inorganics11070313>

Academic Editor: Pingwu Du

Received: 7 July 2023

Revised: 14 July 2023

Accepted: 17 July 2023

Published: 24 July 2023



Copyright: © 2023 by the authors. Licensee MDPI, Basel, Switzerland. This article is an open access article distributed under the terms and conditions of the Creative Commons Attribution (CC BY) license (<https://creativecommons.org/licenses/by/4.0/>).

high-temperature relative equilibrium populations of the five Pr@C₈₂ IPR isomers with the lowest potential energy, employing both the enthalpy and entropy parts of the Gibbs energy in simulations of the isomeric equilibrium populations under supposed fullerene synthesis conditions.

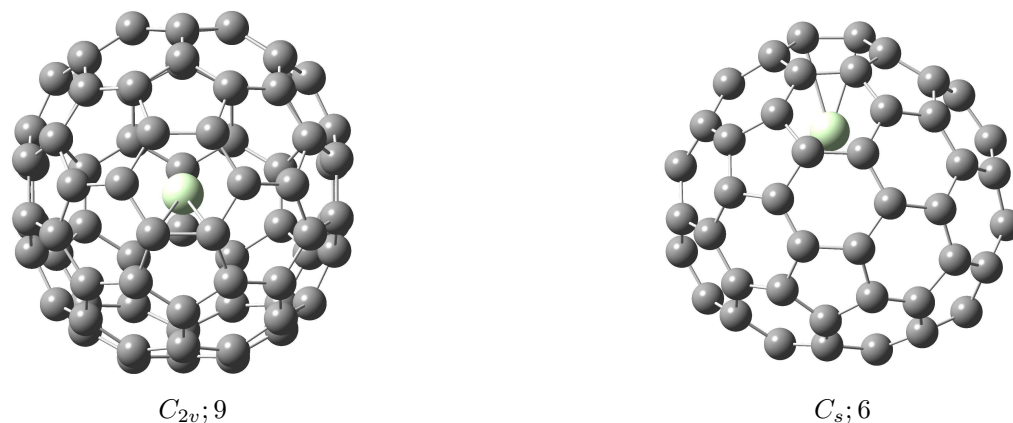


Figure 1. The B3LYP/6-31G*~SDD-optimized structures of the two most populated Pr@C₈₂ isomers, Pr@C_{2v};9-C₈₂ (**left**), Pr@C_s;6-C₈₂ (**right**) (the shortest Pr-C contact is indicated by a link).

2. Calculations

The calculations started with the molecular geometry optimization of the considered isomers, which was performed in a combined atomic basis set—the standard 3-21G basis [27] for carbon atoms and the SDD basis [28] with the SDD effective core potential for praseodymium (labeled 3-21G~SDD). We applied density functional theory (DFT) treatments employing Becke's three-parameter functional [29] combined with the Lee–Yang–Parr non-local correlation functional [30]—the unrestricted B3LYP/3-21G~SDD treatment. Moreover, the B3LYP/3-21G~SDD pre-optimized structures were improved further with the standard 6-31G* basis set [31] for carbon atoms—the B3LYP/6-31G*~SDD approach. The calculations were carried out for the quartet electronic state, as the multiplicity produced significantly lower energy at the considered computational levels than the doublet and sextet electronic states. The geometry optimizations were carried out with the analytical energy gradient. All nine [9] IPR C₈₂ cages were subjected to geometry optimizations. The geometry optimizations with both the B3LYP/3-21G~SDD and B3LYP/6-31G*~SDD treatments identified five isomers (Table 1) with sufficiently low potential energy. All other Pr@C₈₂ IPR isomers were, according to the B3LYP/6-31G*~SDD treatment, located 19 kcal/mol or more higher than the lowest-energy species Pr@C_{2v};9-C₈₂. Their energy separation (in combination with the entropy terms) produced already insignificant relative equilibrium concentrations. Further on, the inter-isomeric energetics was still improved by applying a yet more advanced B3LYP/6-31+G*~SDD approach (still using the B3LYP/6-31G*~SDD geometries). For the optimized B3LYP/6-31G*~SDD geometries, the vibrational analysis was performed using the harmonic GF scheme with the analytical force–constant matrix F in order to simulate the IR vibrational spectra (Figure 2) and, in particular, to construct the partition functions of the harmonic vibrations for the stability evaluations. The SCF wavefunction stability [32,33] was systematically tested throughout in order to prevent misleading unstable SCF solutions that could produce a physically unsound picture. The calculations were performed with the Gaussian 09 suite of programs [34].

Table 1. Pr@C₈₂ relative potential energies $\Delta E_{pot,rel}$ for the five lowest-energy isomers calculated in the B3LYP/6-31G*~SDD-optimized structures.

Species	$\Delta E_{pot,rel}/\text{kcal}\cdot\text{mol}^{-1}$ B3LYP/6-31G*~SDD	B3LYP/6-31+G*~SDD
C ₂ ;5	17.9	17.3
C _{3v} ;7	13.0	14.2
C _{3v} ;8	7.54	7.37
C _s ;6 ^a	3.46	3.47
C _{2v} ;9 ^a	0.0	0.0

^a See Figure 1.

The relative equilibrium concentrations of m isomers are described as mole fractions x_i that can be expressed [35,36] through their partition functions q_i and the enthalpies at a temperature of absolute zero or ground-state energies $\Delta H_{0,i}^0$ (i.e., the relative potential energies corrected for the vibrational zero-point energies) by a master formula:

$$x_i = \frac{q_i \exp[-\Delta H_{0,i}^0/(RT)]}{\sum_{j=1}^m q_j \exp[-\Delta H_{0,j}^0/(RT)]}, \quad (1)$$

where R is the gas constant and T is the absolute temperature. Equation (1) is a rigorous formula that can be obtained [35] using statistical thermodynamics with the standard isomeric Gibbs energies under the conditions of the inter-isomeric thermodynamic equilibrium. The rotational-vibrational components of the partition functions were approximated [36] by the conventional rigid-rotor and harmonic-oscillator (RRHO) approach. Frequency scaling was not applied as it was not significant for the x_i values at high temperatures [37]. Moreover, the chirality contribution [38] was considered accordingly (the partition function q_i for a pair of enantiomers was doubled). The temperatures at which fullerene or metallofullerene electric-arc synthesis takes place are not precisely known; however, recent observations [39] suggest that it takes place somewhere around a temperature of 1500 K. Hence, the values discussed in this report were calculated for this particular temperature region.

Moreover, an adjusted [23,40] RRHO treatment for the description of the metal motions was applied, considering findings [41] suggesting that the encapsulated metal atoms can exercise large-amplitude vibrational motions, in particular at higher temperatures (if the motions are not restricted by derivatizations of cages [42]). It could be expected that if the metal was relatively free, then, at sufficiently elevated temperatures, its motions in different endohedral cages would provide a similar contribution to the overall partition functions. Such similar contributions would consequently be mutually canceled out in Equation (1). This approximation has been called [23,40] the floating, fluctuating, or free encapsulation model (FEM). The FEM treatment consists of two steps. The first step is the suppression of the three lowest vibrational frequencies (which belong to the metal vibrations inside the cage). The second step deals with the symmetries of the cages—they should be taken as the highest topologically possible terms, reflecting the averaging influence of the large-amplitude motions upon the symmetries. For example, with the Pr@C₈₂ IPR isomer related to the C_{2v};9 cage (Table 1), the C_{2v} symmetry is indeed applied in the FEM treatment, in spite of the fact that its static [43] symmetry (i.e., derived from the geometry optimization) is only C_s or even C₁ (Figure 1). The FEM approach is generally known to produce better agreement [23,40] with observed data than the simple RRHO treatment. The FEM approach was thus also applied in this report.

Table 2. The selected characteristics of the five lowest-energy Pr@C₈₂ isomers—the closest Pr-C contact ^a r_{Pr-C} , the Mulliken charge ^b on Pr q_{Pr} , and the lowest vibrational frequency ^a ω_{low} .

Species	$r_{Pr-C}/\text{\AA}$	q_{Pr}	$\omega_{low} / \text{cm}^{-1}$
C ₂ ;5	2.512	2.449	39.3
C _{3v} ;7	2.516	2.293	17.6
C _{3v} ;8	2.476	2.462	22.3
C _s ;6 ^c	2.500	2.337	20.5
C _{2v} ;9 ^c	2.549	2.364	15.8

^a B3LYP/6-31G*~SDD terms. ^b B3LYP/3-21G~SDD terms. ^c See Figure 1.

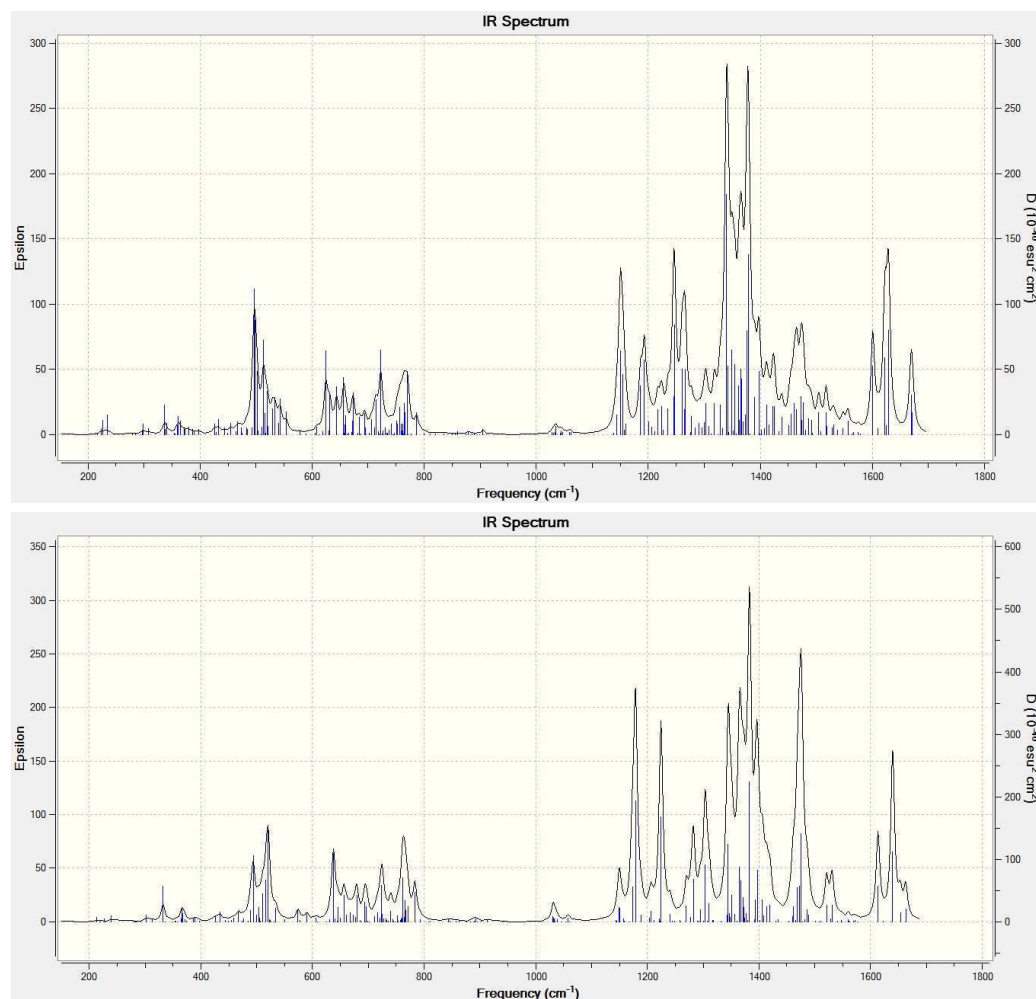


Figure 2. B3LYP/6-31G*~SDD-calculated IR spectrum of the Pr@C_{2v};9-C₈₂ (bottom) and Pr@C_s;6-C₈₂ (top) isomers.

3. Results and Discussion

The Pr@C₈₂ relative isomeric energetics calculated in the two selected approaches (namely, the relative potential energy without the inclusion of the zero-point vibrational energies) for the five lowest-energy isomers selected from the nine [9,44] IPR-satisfying C₈₂ cages are presented in Table 1. The lowest-energy Pr@C₈₂ isomer was the C_{2v};9 species, followed at 3 kcal/mol higher by the C_s;6 endohedral species (Figure 1). Then, C_{3v};8 and C_{3v};7 were located about 7 and 14 kcal/mol above the C_{2v};9 stabilomer, respectively. It should be noted that the B3LYP/6-31G*~SDD and B3LYP/6-31+G*~SDD relative energies were similar. The five species from Table 1 were subjected to equilibrium thermodynamic analysis.

Table 2 presents selected calculated molecular parameters for the five lowest-potential-energy Pr@C₈₂ species. The B3LYP/6-31G*~SDD calculated shortest distances r_{Pr-C} between Pr and the carbon cages at around 2.5 Å, which were thus similar to those previously reported for other C₈₂-based endohedrals [9,15,44]. Interestingly, the calculated position of the Pr atom in Pr@C_{2v};9-C₈₂ (i.e., under a hexagonal ring) is also known for other systems [9]. The lowest harmonic vibrational frequencies ω_{low} in Table 1 reflect the relatively free motions of the encapsulated metals in metallofullerenes. B3LYP/3-21G~SDD produced Mulliken atomic charges q_{Pr} on Pr are close to 2.4 (electron elementary charge). It should be stressed that the Mulliken atomic charges from the 3-21G~SDD basis are known to produce [25] for metallofullerenes good agreement with experimental charges [45] (which is not the case for, e.g., the 6-31G*~SDD level). In addition, there are deeper physical reasons [46–49] why extended bases should not be used for Mulliken charges (as the latter can sometimes produce rather unphysical charges [47]). As for yet another basis-set effect, let us also mention that, as we were only dealing with isomers, there was no need to consider the basis set superposition error (BSSE) [49]. The BSSE correction is indeed important for association processes in order to assure that all the components are treated in the same basis set. In a set of isomers, however, the basis set used is the same for all the species, and therefore the total energies do not require a correction of the BSSE type. If such a treatment was still performed, there would be a relatively constant additive term that would then cancel out in Equation (1).

Figure 3 gives the key results of this report—the temperature dependencies of the relative equilibrium concentrations for the five lowest-potential-energy Pr@C₈₂ isomers at moderate and high temperatures. The presented relative isomeric populations were obtained with the FEM approach. In any case, at very low temperatures, the species with the lowest $\Delta H_{0,i}^o$ had to be the most populated, i.e., the Pr@C_{2v};9-C₈₂ isomer. However, the second (Pr@C_s;6-C₈₂) and, somewhat, the third (Pr@C_{3v};8-C₈₂) lowest-potential-energy isomers showed a rapid increase in their relative populations, while the remaining isomers were negligible. At the suggested [39] representative temperature of 1500 K for fullerene synthesis, the relative equilibrium populations were 59.3, 34.9, 4.8, 0.3, and 0.8% for the C_{2v};9, C_s;6, C_{3v};8, C_{3v};7, and C₂;5 isomers, respectively. Interestingly, in a stability evaluation without the entropic part (i.e., when just the simple Boltzmann factors [35,36] were considered), the relative isomeric populations were rather different: 71.0, 22.2, 6.0, 0.6, and 0.2% for the C_{2v};9, C_s;6, C_{3v};8, C_{3v};7, and C₂;5 species, respectively.

Overall, the calculations agreed with the observations [3–6] for two isomers, major Pr@C_{2v};9-C₈₂ and minor Pr@C_s;6-C₈₂. Their observed [6] population ratio has been reported as Pr@C_{2v};9-C₈₂ : Pr@C_s;6-C₈₂ = 2.5. In our calculations, the population ratio was achieved at a quite reasonable synthetic temperature of 1130 K. Still, it is not known how close the experiments were to the inter-isomeric equilibrium predicted by the thermodynamic treatment. For the interpretation of the observations, it is also of interest that the calculations predicted just two significant isomers, while the populations of the other species were rather negligible. The calculated IR spectra (Figure 2) should also be of use for the identification of the two isomers.

The reported results presented similarities with the previous calculations [12,23,50–54] for other C₈₂-based metallofullerenes with a similar metal-to-cage charge transfer—in particular [12,23], La@C₈₂. The similarities originated from the fact that metallofullerenes are not stabilized by some new covalent bond but instead formed by an ionic bond [55–59]. It should be mentioned that experimental populations can depend on the metal sources used [60]. This aspect can be related to catalytic and kinetic factors [61–63] and indicates the variable levels to which the expected inter-isomeric thermodynamic equilibrium could actually be obtained in the synthesis. Yet another factor is the solubility [64–66] of individual isomers in the selected extraction solvents. In conclusion, the Pr@C₈₂ results provide more evidence of the good applicability of the Gibbs energy approach to isomeric populations, thus supporting further studies of this type into yet more complex nanocarbon isomeric sets [67–71].

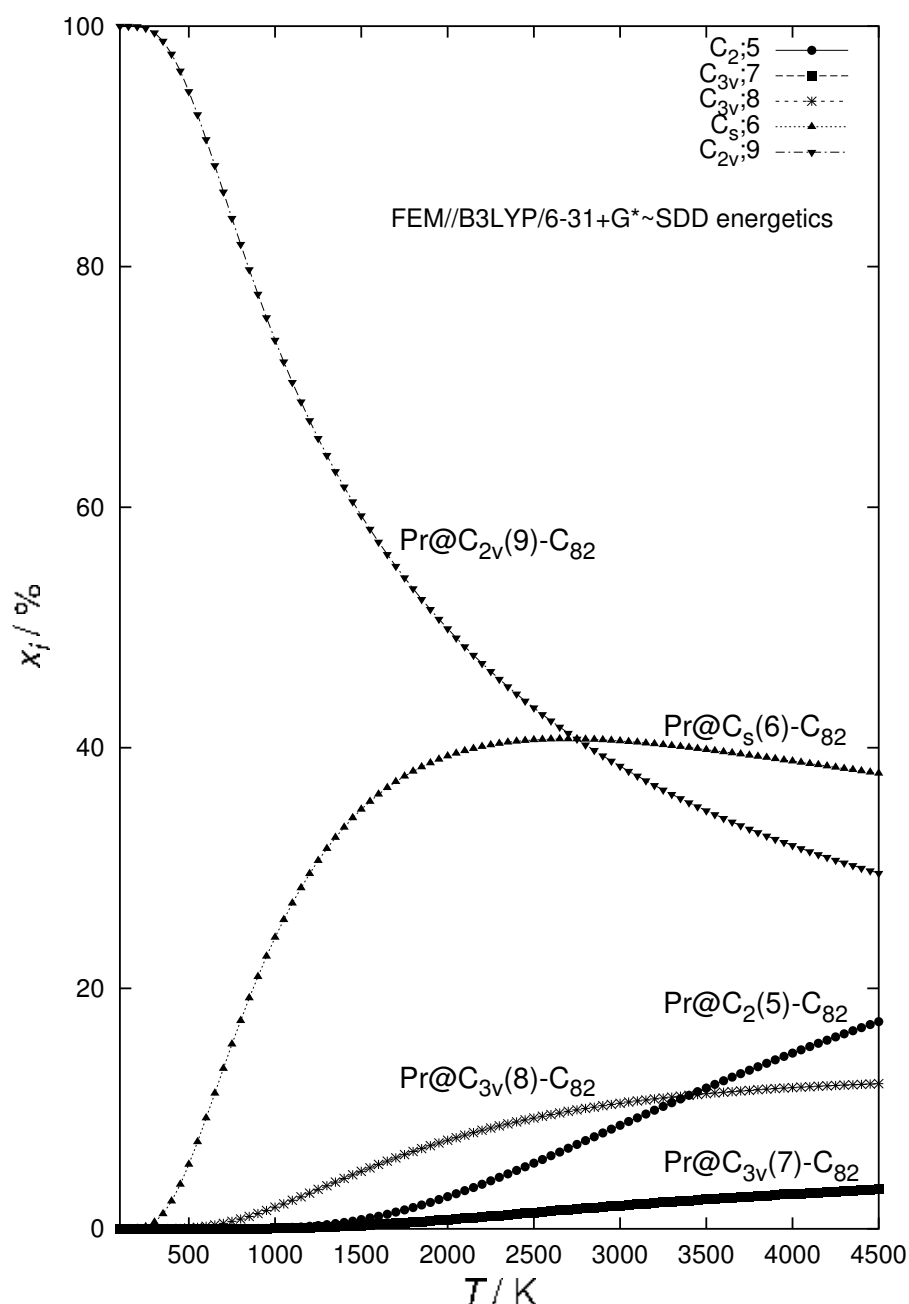


Figure 3. The relative populations of the Pr@C₈₂ isomers based on the FEM treatment with the B3LYP/6-31+G*~SDD energetics and B3LYP/6-31G*~SDD entropy.

Author Contributions: The authors contributed equally to this article. All authors have read and agreed to the published version of the manuscript.

Funding: The reported research was supported by the National Natural Science Foundation of China (21925104 and 92261204); the Hubei Provincial Natural Science Foundation of China (No. 2021CFA020); the International Cooperation Key Project of the Science and Technology Department of Shaanxi; and the Charles University Centre of Advanced Materials/CUCAM (CZ.02.1.01/0.0/0.0/15 003/0000417) and the MetaCentrum ((LM2010005) and CERIT-SC (CZ.1.05/3.2.00/08.0144) computing facilities. The initial phase of the research was also supported by the Alexander von Humboldt-Stiftung and Max Planck Institut für Chemie (Otto Hahn Institut).

Data Availability Statement: Not applicable.

Conflicts of Interest: The authors declare no conflict of interest.

References

1. Wang, W.; Ding, J.; Yang, S.; Li, X.-Y. Electrochemical Properties of 4f-block metallofullerenes. In *Fullerenes. Recent Advances in the Chemistry and Physics of Fullerenes and Related Materials*; Kadish, K.M., Ruoff, R.S., Eds.; Electrochemical Society: Pennington, Australia, 1997; Volume 4, pp. 417–428.
2. Sun, D.Y.; Huang, H.J.; Yang, S.H.; Liu, Z.Y.; Liu, S.Y. Synthesis and characterization of a water-soluble endohedral metallofullerol. *Chem. Mater.* **1999**, *11*, 1003–1006. [[CrossRef](#)]
3. Akasaka, T.; Okubo, S.; Wakahara, T.; Yamamoto, K.; Kato, T.; Suzuki, T.; Nagase, S.; Kobayashi, K. Isolation and characterization of a Pr@C₈₂ isomer. In *Recent Advances in the Chemistry and Physics of Fullerenes and Related Materials*; Kamat, P.V., Guldi, D.M., Kadish, K.M., Eds.; Electrochemical Society: Pennington, Australia, 1999; Volume 7, pp. 771–778.
4. Akasaka, T.; Okubo, S.; Kondo, M.; Maeda, Y.; Wakahara, T.; Kato, T.; Suzuki, T.; Yamamoto, K.; Kobayashi, K.; Nagase, S. Isolation and characterization of two Pr@C₈₂ isomers. *Chem. Phys. Lett.* **2000**, *319*, 153–156. [[CrossRef](#)]
5. Wakahara, T.; Okubo, S.; Kondo, M.; Maeda, Y.; Akasaka, T.; Waelchli, M.; Kako, M.; Kobayashi, K.; Nagase, S.; Kato, T.; et al. Ionization and structural determination of the major isomer of Pr@C₈₂. *Chem. Phys. Lett.* **2002**, *360*, 235–239. [[CrossRef](#)]
6. Hosokawa, T.; Fujiki, S.; Kuwahara, E.; Kubozono, Y.; Kitagawa, H.; Fujiwara, A.; Takenobu, T.; Iwasa, Y. Electronic properties for the C_{2v} and C_s isomers of Pr@C₈₂ studied by Raman, resistivity and scanning tunneling microscopy/spectroscopy. *Chem. Phys. Lett.* **2004**, *395*, 78–81. [[CrossRef](#)]
7. Nagano, T.; Kuwahara, E.; Takayanagi, T.; Kubozono, Y.; Fujiwara, A. Fabrication and characterization of field-effect transistor device with C_{2v} isomer of Pr@C₈₂. *Chem. Phys. Lett.* **2005**, *409*, 187–191. [[CrossRef](#)]
8. Katayanagi, H.; Kafle, B.P.; Kou, J.; Mori, T.; Mitsuke, K.; Takabayashi, Y.; Kuwahara, E.; Kubozono, Y.J. The 4d-4f dipole resonance of the Pr atom in an endohedral metallofullerene, Pr@C₈₂. *J. Quant. Spectrosc. Rad. Trans.* **2008**, *109*, 1590–1598. [[CrossRef](#)]
9. Slanina, Z.; Uhlík, F.; Feng, L.; Adamowicz, L. Calculated relative populations of Sm@C₈₂ isomers. *Fullerenes Nanotub. Carbon Nanostruct.* **2018**, *26*, 233–238. [[CrossRef](#)]
10. Fowler, P.W.; Manolopoulos, D.E. *An Atlas of Fullerenes*; Clarendon Press: Oxford, UK, 1995.
11. Slanina, Z.; Lee, S.-L.; Kobayashi, K.; Nagase, S. AM1 computed thermal effects within the nine isolated-pentagon-rule isomers of C₈₂. *J. Mol. Struct.* **1995**, *339*, 89–93. [[CrossRef](#)]
12. Slanina, Z.; Kobayashi, K.; Nagase, S. Ca@C₈₂ isomers: Computed temperature dependency of relative concentrations. *J. Chem. Phys.* **2004**, *120*, 3397–3400. [[CrossRef](#)]
13. Slanina, Z.; Kobayashi, K.; Nagase, S. Computed temperature development of the relative stabilities of La@C₈₂ isomers. *Chem. Phys. Lett.* **2004**, *388*, 74–78. [[CrossRef](#)]
14. Suzuki, M.; Slanina, Z.; Mizorogi, N.; Lu, X.; Nagase, S.; Olmstead, M.M.; Balch, A.L.; Akasaka, T. Single-crystal X-ray diffraction study of three Yb@C-82 isomers cocrystallized with Ni-II(octaethylporphyrin). *J. Am. Chem. Soc.* **2012**, *134*, 18772–18778. [[CrossRef](#)]
15. Slanina, Z.; Uhlík, F.; Lee, S.-L.; Suzuki, M.; Lu, X.; Mizorogi, N.; Nagase, S.; Akasaka, T. Calculated temperature development of the relative stabilities of Yb@C₈₂ isomers. *Fullerenes Nanotub. Carbon Nanostruct.* **2014**, *22*, 147–154. [[CrossRef](#)]
16. Hu, Z.; Hao, Y.; Slanina, Z.; Gu, Z.; Shi, Z.; Uhlík, F.; Zhao, Y.; Feng, L. Popular C₈₂ fullerene cage encapsulating a divalent metal ion Sm²⁺: Structure and electrochemistry. *Inorg. Chem.* **2015**, *54*, 2103–2108. [[CrossRef](#)]
17. Slanina, Z.; Lee, S.-L.; Adamowicz, L. C₈₀, C₈₆, C₈₈: Semiempirical and ab initio SCF calculations. *Int. J. Quantum. Chem.* **1997**, *63*, 529–535. [[CrossRef](#)]
18. Slanina, Z.; Uhlík, F. Temperature dependence of the Gibbs energy ordering of isomers of Cl₂O₂. *J. Phys. Chem.* **1991**, *95*, 5432–5434. [[CrossRef](#)]
19. Slanina, Z.; Zhao, X.; Lee, S.-L.; Ōsawa, E. C₉₀-Temperature effects on relative stabilities of the IPR isomers. *Chem. Phys.* **1997**, *219*, 193–200. [[CrossRef](#)]
20. Uhlík, F.; Slanina, Z.; Ōsawa, E. C₇₈ IPR fullerenes: Computed B3LYP/6-31G*//HF/3-21G temperature-dependent relative concentrations. *Eur. Phys. J. D* **2001**, *16*, 349–352. [[CrossRef](#)]
21. Slanina, Z.; Zhao, X.; Uhlík, F.; Lee, S.-L.; Adamowicz, L. Computing enthalpy-entropy interplay for isomeric fullerenes. *Int. J. Quantum Chem.* **2004**, *99*, 640–653. [[CrossRef](#)]
22. Slanina, Z.; Lee, S.-L.; Adamowicz, L.; Uhlík, F.; Nagase, S. Computed structure and energetics of La@C₆₀. *Int. J. Quantum Chem.* **2005**, *104*, 272–277. [[CrossRef](#)]
23. Slanina, Z.; Lee, S.-L.; Uhlík, F.; Adamowicz, L.; Nagase, S. Computing relative stabilities of metallofullerenes by Gibbs energy treatments. *Theor. Chem. Acc.* **2007**, *117*, 315–322. [[CrossRef](#)]
24. Wang, Y.; Morales-Martínez, R.; Zhang, X.; Yang, W.; Wang, Y.; Rodríguez-Forteza, A.; Poblet, J.M.; Feng, L.; Wang, S.; Chen, N. Unique four-electron metal-to-cage charge transfer of Th to a C₈₂ fullerene cage: Complete structural characterization of Th@C_{3v}(8)-C₈₂. *J. Am. Chem. Soc.* **2017**, *139*, 5110–5116. [[CrossRef](#)] [[PubMed](#)]
25. Slanina, Z.; Uhlík, F.; Nagase, S.; Akasaka, T.; Adamowicz, L.; Lu, X. Eu@C₇₂: Computed comparable populations of two non-IPR isomers. *Molecules* **2017**, *22*, 1053. [[CrossRef](#)]
26. Zhao, Y.; Li, M.; Zhao, R.; Zhao, P.; Yuan, K.; Li, Q.; Zhao, X. Unmasking the optimal isomers of Ti₂C₈₄: Ti₂C₂@C₈₂ Instead of Ti₂C₈₄. *J. Phys. Chem. C* **2018**, *122*, 13148–13155. [[CrossRef](#)]
27. Binkley, J.S.; Pople, J.A.; Hehre, W.J. Self-consistent molecular orbital methods. 21. Small split-valence basis sets for first-row elements. *J. Am. Chem. Soc.* **1980**, *102*, 939–947. [[CrossRef](#)]

28. Cao, X.Y.; Dolg, M. Segmented contraction scheme for small-core lanthanide pseudopotential basis sets. *J. Mol. Struct.* **2002**, *581*, 139–147. [CrossRef]
29. Becke, A.D. Density-functional thermochemistry. III. The role of exact exchange. *J. Chem. Phys.* **1993**, *98*, 5648–5652. [CrossRef]
30. Lee, C.; Yang, W.; Parr, R.G. Development of the Colle-Salvetti correlation-energy formula into a functional of the electron density. *Phys. Rev. B* **1988**, *37*, 785–789. [CrossRef]
31. Hehre, W.J.; Ditchfield, R.; Pople, J.A. Self-consistent molecular orbital methods. 12. Further extensions of Gaussian-type basis sets for use in molecular-orbital studies of organic-molecules. *J. Chem. Phys.* **1972**, *56*, 2257–2261. [CrossRef]
32. Schlegel, H.B.; McDouall, J.J.W. Do you have SCF stability and convergence problems? In *Computational Advances in Organic Chemistry*; Ögretir, C., Csizmadia, I.G., Eds.; Kluwer: Dordrecht, The Netherlands, 1991; pp. 167–185.
33. Slanina, Z.; Uhlík, F.; Adamowicz, L. Computations of model narrow nanotubes closed by fragments of smaller fullerenes and quasi-fullerenes. *J. Mol. Graph. Mod.* **2003**, *21*, 517–522. [CrossRef]
34. Frisch, M.J.; Trucks, G.W.; Schlegel, H.B.; Scuseria, G.E.; Robb, M.A.; Cheeseman, J.R.; Scalmani, G.; Barone, V.; Mennucci, B.; Petersson, G.A.; et al. *Gaussian 09, Rev. C.01*; Gaussian Inc.: Wallingford, CT, USA, 2013.
35. Slanina, Z. Equilibrium isomeric mixtures: Potential energy hypersurfaces as originators of the description of the overall thermodynamics and kinetics. *Int. Rev. Phys. Chem.* **1987**, *6*, 251–267. [CrossRef]
36. Slanina, Z. A Program for determination of composition and thermodynamics of the ideal gas-phase equilibrium isomeric mixtures. *Comput. Chem.* **1989**, *13*, 305–311. [CrossRef]
37. Slanina, Z.; Uhlík, F.; Zerner, M.C. $C_5H_3^+$ isomeric structures: Relative stabilities at high temperatures. *Rev. Roum. Chim.* **1991**, *36*, 965–974.
38. Slanina, Z.; Adamowicz, L. On relative stabilities of dodecahedron-shaped and bowl-shaped structures of C_{20} . *Thermochim. Acta* **1992**, *205*, 299–306. [CrossRef]
39. Cross, R.J.; Saunders, M. Transmutation of fullerenes. *J. Am. Chem. Soc.* **2005**, *127*, 3044–3047. [CrossRef]
40. Slanina, Z.; Adamowicz, L.; Kobayashi, K.; Nagase, S. Gibbs energy-based treatment of metallofullerenes: $Ca@C_{72}$, $Ca@C_{74}$, $Ca@C_{82}$, and $La@C_{82}$. *Mol. Simul.* **2005**, *31*, 71–77. [CrossRef]
41. Akasaka, T.; Nagase, S.; Kobayashi, K.; Walchli, M.; Yamamoto, K.; Funasaka, H.; Kako, M.; Hoshino, T.; Erata, T. ^{13}C and ^{139}La NMR studies of $La_2@C_{80}$: First evidence for circular motion of metal atoms in endohedral dimetallofullerenes. *Angew. Chem. Int. Ed.* **1997**, *36*, 1643–1645. [CrossRef]
42. Kobayashi, K.; Nagase, S.; Maeda, Y.; Wakahara, T.; Akasaka, T. $La_2@C_{80}$: Is the circular motion of two La atoms controllable by exohedral addition? *Chem. Phys. Lett.* **2003**, *374*, 562–566. [CrossRef]
43. Slanina, Z. *Contemporary Theory of Chemical Isomerism*; Academia: Prague, Czech Republic; D. Reidel Publ. Comp.: Dordrecht, The Netherlands, 1986; pp. 21–23.
44. Slanina, Z.; Uhlík, F.; Bao, L.; Akasaka, T.; Lu, X.; Adamowicz, L. Calculated relative populations for the $Eu@C_{82}$ isomers. *Chem. Phys. Lett.* **2019**, *726*, 29–33. [CrossRef]
45. Takata, M.; Nishibori, E.; Sakata, M.; Shinohara, H. Charge density level structures of endohedral metallofullerenes determined by synchrotron radiation powder method. *New Diam. Front. Carb. Technol.* **2002**, *12*, 271–286.
46. Hehre, W.J. *A Guide to Molecular Mechanics and Quantum Chemical Calculations*; Wavefunction: Irvine, CA, USA, 2003; p. 435.
47. Jensen, F. *Introduction to Computational Chemistry*; Wiley: Chichester, UK, 2017; p. 319.
48. Campanera, J.M.; Bo, C.; Poblet, J.M. General rule for the stabilization of fullerene cages encapsulating trimetallic nitride templates. *Angew. Chem. Int. Ed.* **2005**, *44*, 7230–7233. [CrossRef]
49. Slanina, Z.; Uhlík, F.; Pan, C.; Akasaka, T.; Lu, X.; Adamowicz, L. Computed stabilization for a giant fullerene endohedral: $Y_2C_2@C_1(1660)-C_{108}$. *Chem. Phys. Lett.* **2018**, *710*, 147–149. [CrossRef]
50. Slanina, Z.; Uhlík, F.; Lee, S.-L.; Nagase, S. Structural and bonding features of $Z@C_{82}$ ($Z = Al, Sc, Y, La$) endohedrals. *J. Comput. Meth. Sci. Engn.* **2010**, *10*, 569–574. [CrossRef]
51. Slanina, Z.; Uhlík, F.; Shen, W.; Akasaka, T.; Lu, X.; Adamowicz, L. Calculations of the relative populations of $Lu@C_{82}$ isomers. *Nanotub. Carbon Nanostruct.* **2019**, *27*, 710–714. [CrossRef]
52. Slanina, Z.; Uhlík, F.; Akasaka, T.; Lu, X.; Adamowicz, L. Calculated relative thermodynamic stabilities of the $Gd@C_{82}$ isomers. *ECS J. Solid State Sci. Technol.* **2021**, *10*, 071013-1–071013-4. [CrossRef]
53. Meng, Q.Y.; Morales-Martínez, R.; Zhuang, J.X.; Yao, Y. R.; Wang, Y.F.; Feng, L.; Poblet, J.M.; Rodríguez-Fortea, A.; Chen, N. Synthesis and characterization of two isomers of $Th@C_{82}$: $Th@C_{2v}(9)-C_{82}$ and $Th@C_2(5)-C_{82}$. *Inorg. Chem.* **2021**, *60*, 11496–11502. [CrossRef]
54. Slanina, Z.; Uhlík, F.; Feng, L.; Adamowicz, L. $Ho@C_{82}$ metallofullerene: Calculated isomeric composition. *ECS J. Solid State Sci. Technol.* **2022**, *11*, 053018-1–053018-4. [CrossRef]
55. Andreoni, W.; Curioni, A. Freedom and constraints of a metal atom encapsulated in fullerene cages. *Phys. Rev. Lett.* **1996**, *77*, 834–837. [CrossRef]
56. Popov, A.A.; Dunsch, L. Bonding in endohedral metallofullerenes as studied by quantum theory of atoms in molecules. *Chem. Eur. J.* **2009**, *15*, 9707–9729. [CrossRef]
57. Slanina, Z.; Uhlík, F.; Lee, S.-L.; Adamowicz, L.; Akasaka, T.; Nagase, S. Computed stabilities in metallofullerene series: $Al@C_{82}$, $Sc@C_{82}$, $Y@C_{82}$, and $La@C_{82}$. *Int. J. Quant. Chem.* **2011**, *111*, 2712–2718. [CrossRef]

58. Rodríguez-Forteza, A.; Balch, A.L.; Poblet, J.M. Endohedral metallofullerenes: A unique host-guest association. *Chem. Soc. Rev.* **2011**, *40*, 3551–3563. [[CrossRef](#)]
59. Popov, A.A.; Yang, S.; Dunsch, L. Endohedral fullerenes. *Chem. Rev.* **2013**, *113*, 5989–6113. [[CrossRef](#)]
60. Yang, H.; Yu, M.; Jin, H.; Liu, Z.; Yao, M.; Liu, B.; Olmstead, M.M.; Balch, A.L. Isolation of three isomers of Sm@C₈₄ and X-ray crystallographic characterization of Sm@D_{3d}(19)-C₈₄ and Sm@C₂(13)-C₈₄. *J. Am. Chem. Soc.* **2012**, *134*, 5331 [[CrossRef](#)]
61. Slanina, Z.; Zhao, X.; Uhlík, F.; Ozawa, M.; Osawa, E. Computational modelling of the metal and other elemental catalysis in the Stone-Wales fullerene rearrangements. *J. Organomet. Chem.* **2000**, *599*, 57–61. [[CrossRef](#)]
62. Hao, Y.; Feng, L.; Xu, W.; Gu, Z.; Hu, Z.; Shi, Z.; Slanina, Z.; Uhlík, F. Sm@C_{2v}(19I38)-C₇₆: A Non-IPR Cage Stabilized by a Divalent Metal Ion. *Inorg. Chem.* **2015**, *54*, 4243–4248. [[CrossRef](#)]
63. Hao, Y.; Tang, Q.; Li, X.; Zhang, M.; Wan, Y.; Feng, L.; Chen, N.; Slanina, Z.; Adamowicz, L.; Uhlík, F. Isomeric Sc₂O@C₇₈ related by a single-step Stone–Wales transformation: Key links in an unprecedented fullerene formation pathway. *Inorg. Chem.* **2016**, *55*, 11354–11361. [[CrossRef](#)]
64. Jehlička, J.; Svatoš, A.; Frank, O.; Uhlík, F. Evidence for fullerenes in solid bitumen from pillow lavas of proterozoic age from Mítov (Bohemian Massif, Czech Republic) Geochem. *Cosmochem. Acta* **2003**, *67*, 1495–1506. [[CrossRef](#)]
65. Lian, Y.; Shi, Z.; Zhou, X.; Gu, Z. Different extraction behaviors between divalent and trivalent endohedral metallofullerenes. *Chem. Mater.* **2004**, *16*, 1704–1714. [[CrossRef](#)]
66. Maeda, Y.; Tsuchiya, T.; Kikuchi, T.; Nikawa, H.; Yang, T.; Zhao, X.; Slanina, Z.; Suzuki, M.; Yamada, M.; Lian, Y.; et al. Effective derivatization and extraction of insoluble missing lanthanum metallofullerenes La@C_{2n} (n = 36–38) with iodobenzene. *Carbon* **2016**, *98*, 67–73. [[CrossRef](#)]
67. An, D.-Y.; Su, J.-G.; Li, C.-H.; Li, J.-Y. Computational studies on the interactions of nanomaterials with proteins and their impacts. *Chin. Phys. B* **2015**, *24*, 120504-1–120504-8. [[CrossRef](#)]
68. Basiuk, V.A.; Tahuilan-Anguiano, D.E. Complexation of free-base and 3d transition metal(II) phthalocyanines with endohedral fullerene Sc₃N@C₈₀. *Chem. Phys. Lett.* **2019**, *722*, 146–152. [[CrossRef](#)]
69. Tahuilan-Anguiano, D.E.; Basiuk, V.A. Complexation of free-base and 3d transition metal(II) phthalocyanines with endohedral fullerenes H@C₆₀, H₂@C₆₀ and He@C₆₀: The effect of encapsulated species. *Diam. Rel. Mat.* **2021**, *118*, 108510-1–108510-5. [[CrossRef](#)]
70. Li, M.; Zhao, R.; Dang, J.; Zhao, X. Theoretical study on the stabilities, electronic structures, and reaction and formation mechanisms of fullerenes and endohedral metallofullerenes. *Coor. Chem. Rev.* **2022**, *471*, 214762-1–214762-12. [[CrossRef](#)]
71. Slanina, Z.; Uhlík, F.; Adamowicz, L. Theoretical predictions of fullerene stabilities. In *Handbook of Fullerene Science and Technology*; Lu, X., Akasaka, T., Slanina, Z., Eds.; Springer: Singapore, 2022; pp. 111–179.

Disclaimer/Publisher's Note: The statements, opinions and data contained in all publications are solely those of the individual author(s) and contributor(s) and not of MDPI and/or the editor(s). MDPI and/or the editor(s) disclaim responsibility for any injury to people or property resulting from any ideas, methods, instructions or products referred to in the content.